MODELING OF RADAR BACKSCATTER FROM ICY AND ROUGH LUNAR CRATERS

Thomas W. Thompson*(1), Eugene A. Ustinov(1), Paul D. Spudis(2), and Brian W. Fessler(2)
(1) Jet Propulsion Laboratory, 4800 Oak Grove Drive, Pasadena, CA 91109, USA, Phone: 818-354-3881, Fax: 818-393-5285, Thomas.W.Thompson@jpl.nasa.gov. (2) Lunar and Planetary Institute, 3600 Bay Area Blvd. Houston, TX 77058

Scientific context: The data from two orbital synthetic aperture radars - the Chandrayaan Mini-RF, which operated at 12.6-cm wavelength (S-band) and the Lunar Reconnaissance Orbiter Mini-RF operating at 12.6 cm and 4.5 cm (X-band) – were designed to map the polar regions of the Moon to search for evidence of presence of ice deposits in the polar shadowed areas [1,2]. The performance and scientific return from these experiments require that we understand the radar backscattering characteristics of the icy lunar regoliths sufficiently well to assess the possibility of frozen volatiles in the surface and shallow subsurface (defined here to depths of about 10 times the wavelength). If ices in the permanently shadowed areas of the lunar poles have physical characteristics similar to the ice on Mercury, Mars and the Galilean satellites, then these deposits will have substantial radar enhancement characterized by a circular polarization ratio (CPR) greater than unity. Here we examine how this distinct CPR signature may be diminished by factors such as a thin regolith covering the ice and the ice occupying small patches within a larger radar pixel. Additionally, we attempt to distinguish between CPRs resulting from the presence of ice and those resulting from wavelength-scale surface roughness from blocky crater ejecta [3].

Specular-Diffuse Scattering Models: Our model for scattering from a lunar surface assumes a mixing model consisting of diffuse and specular components [4]. The specular component results from the surface and sub-surface layers that are smooth to a tenth of a radar wavelength for large (10 wavelengths or more) areas oriented perpendicular to the radar's line-of-sight. The diffuse component, which is associated with either surface roughness (wavelength-sized rocks) or composition (e.g., ice), is assumed to be uniformly bright, with backscatter being proportional to the cosine of the incidence angle. Only diffuse scattering contributes to the same-sense circular (SC) echoes. Diffuse scattering from rocky areas associated with young, rough craters (Erastothenian and Copernican aged) is assumed to have CPRs of unity; ices are assumed to have CPRs of 2 (like those observed on Mercury, Mars and Galilean satellites).

Modeling Results: This modeling was examined for 4 nonpolar fresh craters and 12 polar anomalous craters using LRO Mini-RF 12.6-cm wavelength data. In addition, we examined the craters that have unusual circular polarization ratios (CPRs) that likely result from a double bounce mode of scattering. Backscatter for these craters results from two reflections on the interior crater walls where the sum of the two scattering angles equals 180°. These craters have a characteristic of having enhanced backscatter beyond the far crater wall in the radar images.

Our results, shown in Table 1 and Figure 1, indicate that blocky fresh craters, icy craters, and craters exhibiting double bounce scattering can be separated from each other based on the values of SC enhancement (α) and opposite-sense circular (OC) enhancement (γ), the ratio of α to γ and the weighted sum [$0.12\ \alpha + 0.88\ \gamma$]. The ratio of α to γ is a proxy for CPR; the weighted sum is measure of the total power enhancement. In particular, for craters with a SC enhancement (α) greater than unity:

For Rough (Fresh, Blocky) Craters:
$\alpha > 1.5$; $\gamma > 1.0$ or 1.25
Ratio (α/γ) > 1.25 or 1.5
Weighted Sum > 1.0 or 1.25

For Icy Craters:
$\alpha > 1.0$ or 1.25; $0.5 < \gamma < 1.0$ or 1.25
Ratio (α/γ) > 1.5
0.5 < Weighted Sum < 1.0

For Anomalous, Double Bounce Craters:
$\alpha < 1.0$; $\gamma < 0.5$
Ratio (α/γ) > 1.5
Weighted Sum < 0.5

In summary, these results of our modeling indicate that there are 3 separable classes of craters (Icy, Rough, and Double Bounce) based upon their SC enhancements (α) and OC enhancements (γ), their ratio (α/γ), and weighted sum as shown in Table 1 and Figure 1. Use of these four variables together is a better discriminator than using CPR alone. We are currently refining this classification and intend to produce a map showing the distribution of ice-rich craters at both poles.

References: [1] Spudis P.D. et al. (2009) Current Science (India) 96, 4. [2] Nozette S. et al. (2010) Space Sci. Rev. 150, 285. [3] Spudis P.D. et al. (2010) GRL 37, L06204, doi:10.1029/2009GL042259 [4] Thompson T. W., et al. (2011) *JGR*, **116**, E01006, doi:10.1029/2009JE003368.

Table 1. Results for 4 nonpolar fresh craters and 12 polar anomalous craters examined with the specular-diffuse scattering model of Thompson et al. [4]

Crater	Alpha	Gamma	Ratio	Weighted Sum	Model Fit
Fresh Nonpolar					
Giordano Bruno	4.20	2.02	2.1	2.27	< Rough Surface
Byrgius A	2.36	1.97	1.2	2.02	<< Rough Surface
Euclides - New	1.90	0.93	2.0	1.04	Rough - Patches
Fresh Polar					
Main L	2.69	1.26	2.1	1.43	Rough Surface
Near Rozhdestvensky	1.47	1.12	1.3	1.16	Rough Surface
Icy					
Floor of Peary 1	1.10	0.65	1.7	0.70	Thin Regolith
Floor of Peary 2	1.81	0.80	2.3	0.92	Ice Patches
Rozhdestvensky N	1.31	0.79	1.7	0.85	Ice Patches
Floor of Hermite Cut 1	1.30	0.60	2.2	0.68	Thin Regolith
Floor of Hermite Cut 2	1.77	0.70	2.5	0.82	Ice
Hermite A	1.75	0.49	3.6	0.64	Thin Regolith
Erlanger	1.33	0.36	3.7	0.47	> Thin Regolith
Anomalous/ Double-Bounce					
Byrgius	0.84	0.30	2.8	0.36	Yes
First Rozhdestvensky - Floor	0.65	0.39	1.7	0.42	Likely
Second Rozhdestvensky - Floor	0.88	0.42	2.1	0.47	Likely
Shackleton	0.78	0.50	1.6	0.53	Likely

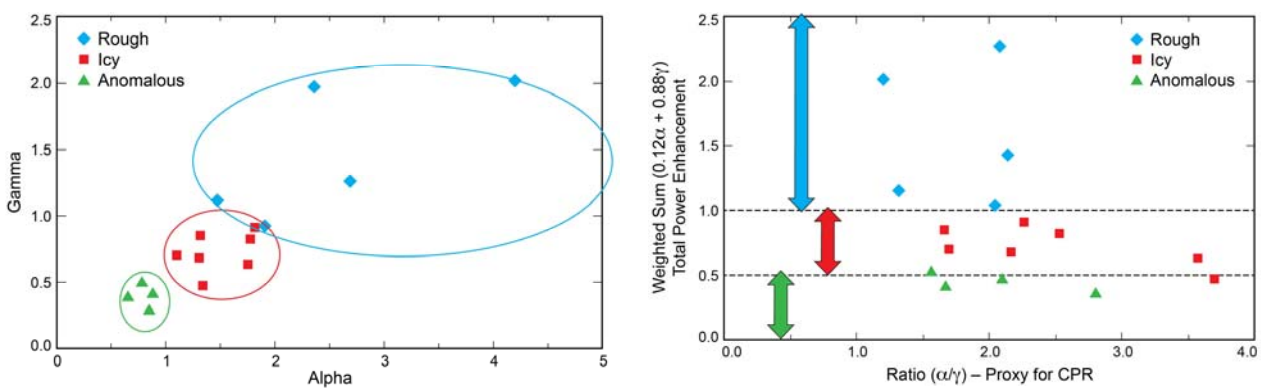

Fig. 1. Scatterplots of α vs. γ (left) and of ratio (α/γ) vs. weighted sum [0.12 α + 0.88 γ] (right) for the 4 nonpolar craters and 12 polar craters studied using LRO Mini-RF 13-cm wavelength data. Ratio (α/γ) is a proxy for CPR; weighted sum is the total power enhancement. There are 3 separable crater classes: Icy, Rough, and Double-Bounce.